MARS
The International Journal of Mars Science and Exploration

MARS INFORMATICS
Open Access Journals

Science

Accumulation and erosion of south polar layered deposits in the Promethei Lingula region, Planum Australe, Mars

Eric J. Kolb[1], Kenneth L. Tanaka[2]

[1]*Dept. of Geological Sciences, Arizona State University, Tempe, AZ, 85287, USA, ekolb@asu.edu;*
[2]*Astrogeology Team, U.S. Geological Survey, Flagstaff, AZ, 86001, USA*

Citation: MARS 2, 1-9, 2006; doi:10.1555/mars.2006.0001
History: Submitted December 4, 2005; Reviewed February 4, 2006; Revised March 13, 2006; Accepted March 31, 2006; Published April 15, 2006
Editor: Jeffrey B. Plescia, Applied Physics Laboratory, Johns Hopkins University
Reviewers: Jeffrey B. Plescia, Applied Physics Laboratory, Johns Hopkins University; Frank P. Seelos, Applied Physics Laboratory, Johns Hopkins University

Abstract

Background: Promethei Lingula, a part of Mars' south polar plateau, Planum Australe, is made up of south polar layered deposits (SPLD) and includes three broad, deep canyons trending perpendicular to the plateau margin and several spiral troughs concentric to the plateau. Two of the canyons, Promethei and Ultimum Chasmata, expose substrate beneath SPLD, and the other canyon displays a variety of erosional landforms within SPLD, including curvilinear, longitudinal grooves (Australe Sulci).

Method: Recent Mars Global Surveyor and Mars Odyssey data sets permit us to map, characterize, and evaluate the region's geologic materials, features, mechanisms, and history.

Results: Our results indicate that aeolian-based SPLD accumulation and erosion were topographically controlled by the rugged Promethei basin rim and other underlying features, leading to dipping beds that define seedling canyons. Formation of the two chasmata included an earlier erosional stage that resulted in SPLD unconformities in chasmata walls. A later erosional episode enlarged and perhaps connected seedling canyons into their present form and carved the spiral troughs. Within the Australe Sulci region, erosion on variably competent SPLD sequences produced longitudinal grooves, domes and asymmetric ridges within gently dipping SPLD (maximum dip <3.0°), and circular mounds of impact-hardened SPLD. Additional SPLD were draped over the surface. Subsequent erosion is largely confined to the chasmata walls and marginal scarp of Promethei Lingula. No evidence is observed for lateral migration of spiral troughs.

Introduction

Roughly half of the south polar Promethei Lingula region on Mars is dissected by curvilinear canyon systems radial to the margin of the Planum Australe plateau and by several smaller, curvilinear trough systems perpendicular to the canyons that are commonly referred to as spiral troughs (Figure 1). Promethei and Ultimum Chasmata are deeper canyons that extend from Planum Australe's margins to its central region. A similarly oriented but shallower canyon marked by Australe Sulci grooves and most of the spiral troughs occur west of the chasmata. Chasma Australe is the largest south polar canyon (not included in this study) and forms the west boundary of Promethei Lingula. The Australe Sulci canyon is similar to Chasma Australe in length, width, and orientation. Australe Sulci consist of dense, parallel sets of curvilinear grooves trending down canyon (also referred to as "Wire Brush" terrain by Koutnik et al. (2005)). The canyon also includes several canyon-transecting sinuous ridges and circular and elongated mounds.

Viking-based geologic mapping of Planum Australe by Tanaka and Scott (1987) delineated residual ice near the pole on top of a single unit of south polar layered deposits (SPLD). Our preliminary Mars Global Surveyor (MGS) and Mars Odyssey (ODY)-based regional mapping (Tanaka and Kolb 2005) divides the SPLD into the Planum Australe 1 and 2 units (Aa_1 and Aa_2, respectively; Figure 1). The Planum

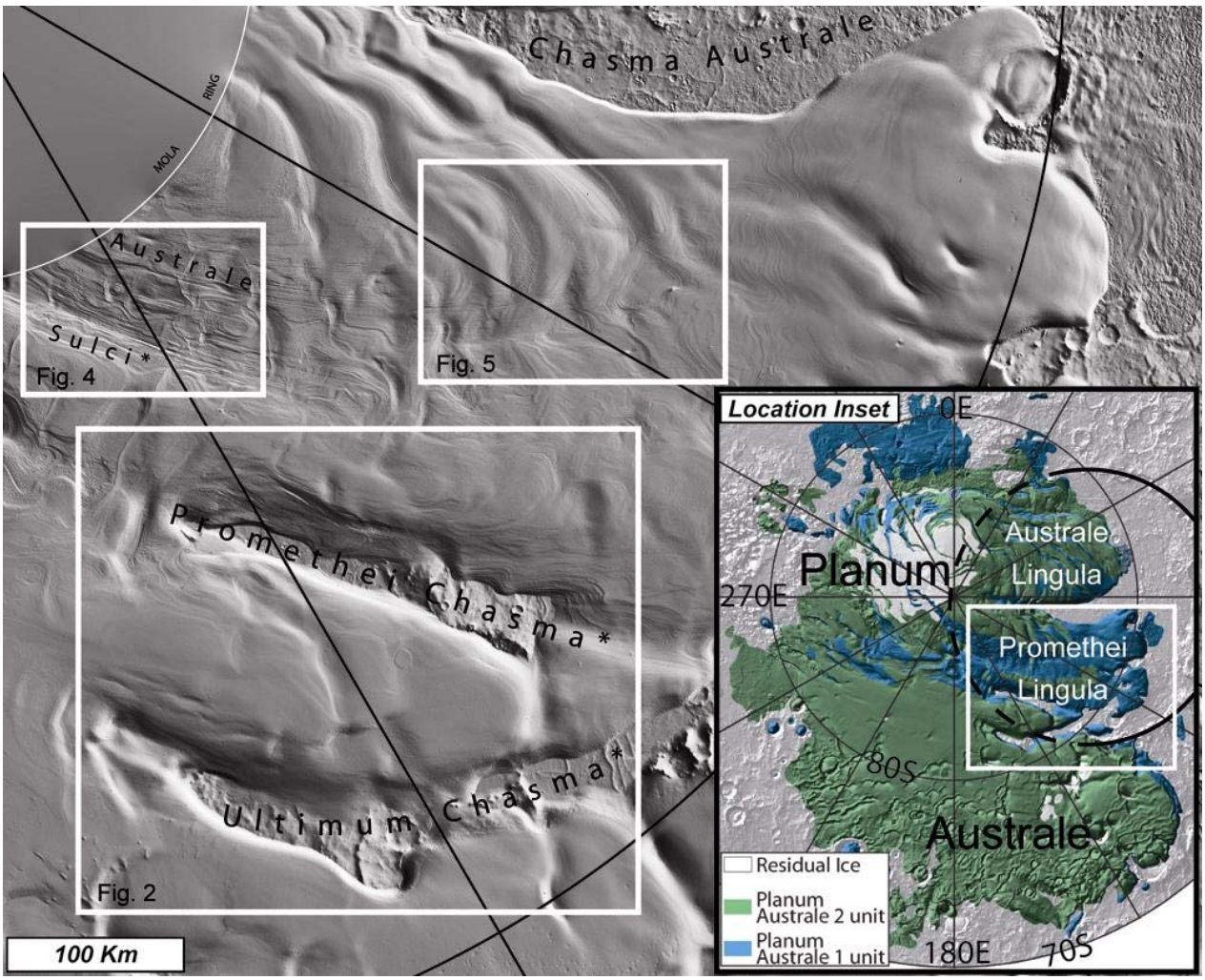

Figure 1. Promethei Lingula region of Planum Australe marked by roughly radial canyons and curvilinear troughs. White rectangles outline regions shown in subsequent figures. "MOLA ring" outlines area of low data resolution. Inset shows extent of Planum Australe 1 and 2 units and residual ice making up Planum Australe, main figure region (white rectangle), and Promethei basin rim (black circle; dashed where buried). MOLA shaded relief base at 115 m/pixel resolution for this and subsequent plan-view figures. (figure1.jpg)

Australe 1 unit comprises most of the volume of the SPLD and is characterized from Mars Orbiter Camera narrow-angle (MOC NA) and Thermal Emission Imaging System (THEMIS) images as evenly bedded sequences of meters-thick layers exposed in canyon and trough walls. Mars Orbiter Laser Altimeter (MOLA) data indicates the unit approaches 2000 m in thickness in the study region. The Planum Australe 2 unit is also comprised of multiple layers that are evenly-bedded although the unit's total thickness is <300 m. Individual layers generally appear slightly thicker than their Planum Australe 1 counterpart and often exhibit moderately to heavily pitted and knobby surfaces. The unit unconformably mantles the eroded topography of the Planum Australe 1 unit and is largely preserved on polar surfaces other than the trough and canyon scarps (Figure 1 inset).

The SPLD apparently formed by deposition of CO_2 and H_2O ice precipitates and atmospheric dust (e.g., Thomas 1992; Mellon 1996). The SPLD surface age is <100 Ma (Herkenhoff and Plaut 2000; Koutnik et al. 2002) and may record variable ice/dust deposition that in turn, result from changing ice stability, water-vapor transport, and dust-storm frequency parameters occurring in response to Mars' cyclical and highly variable obliquity, orbital eccentricity, and precession oscillations (e.g., Thomas 1992).

The analysis of spacecraft data support dissection by katabatic wind as the origin of the polar canyons, the Australe Sulci grooves, and sinuous ridges (Howard 2000; Koutnik et al. 2005). Ablation-driven erosion and redeposition and aeolian erosion of SPLD have been invoked to explain spiral trough development (Howard 1978; Howard 2000). Although glacio-dynamic processes were invoked to explain the dissection of canyons by basal SPLD melting and jökulhlaup-style discharges (e.g., Clifford 1987), the formation of Australe Sulci by ice streaming (Head 2000), and the development of spiral troughs by ductile deformation of the SPLD (e.g., Fisher 1993), we previously concluded that landform assemblages and en- and supra-ice

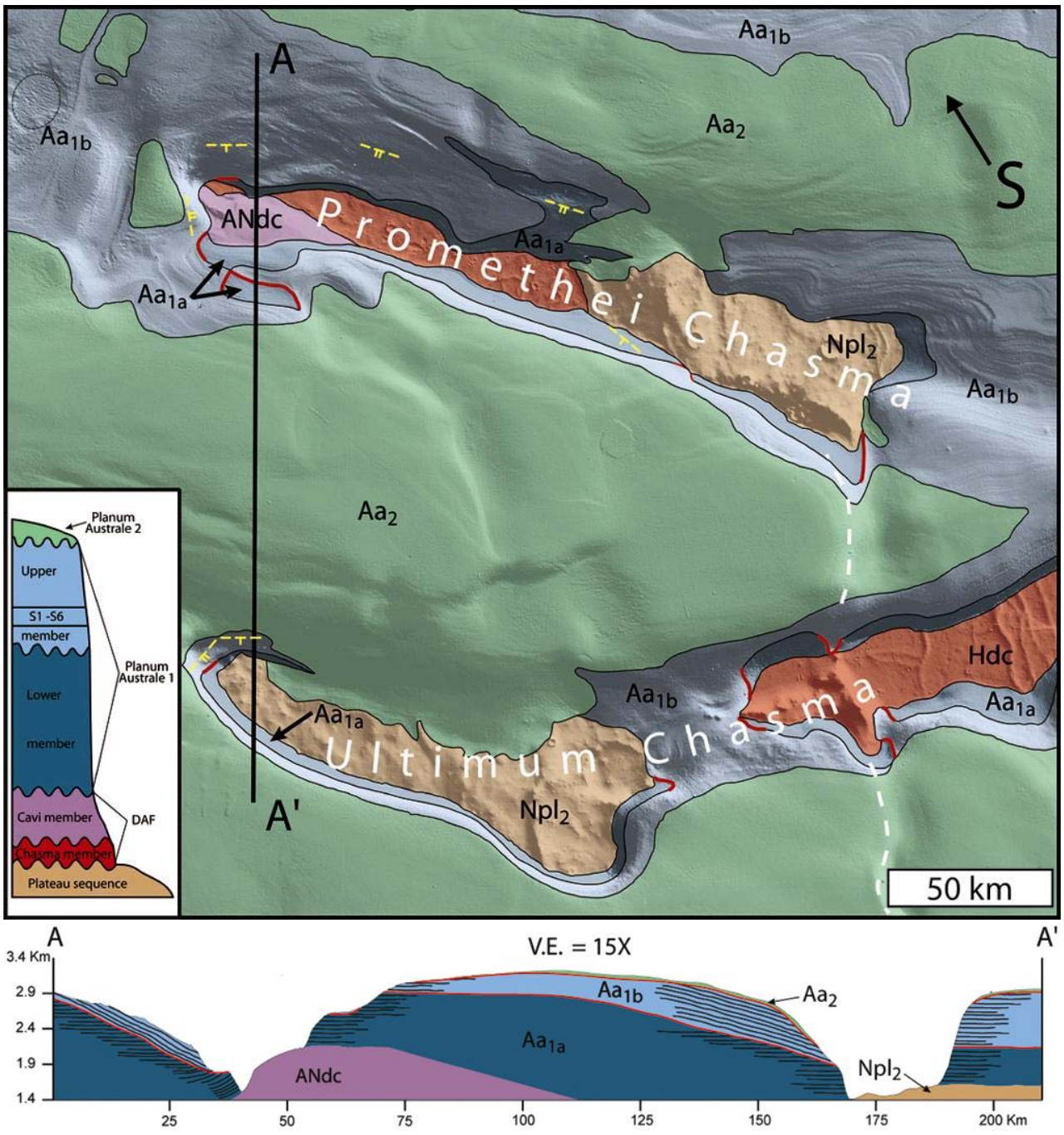

Figure 2. Geologic map, stratigraphic column, and cross-section of Promethei and Ultimum Chasmata. Red lines trace local unconformities that divide Planum Australe 1 into lower and upper members (Aa_{1a} and Aa_{1b}, respectively); also, Planum Australe 2 unit (Aa_2) unconformably overlies Planum Australe 1 units. Relative magnitude of bed dip indicated by number of dip tick marks on strike-and-dip symbols (1 tick = shallow dip, 2 ticks = steeper dip). Floor material includes Noachian impact breccias and associated volcanics (unit Npl_2), and the previously volatile-rich cavi (unit ANdc) and chasma (unit Hdc) members (Kolb and Tanaka 2001) of the Hesperian circum-polar Dorsa Argentea Formation (DAF). Dashed white line traces a northeast-trending trough. (figure2a.jpg, figure2b.jpg)

features diagnostic of any significant glacial deformation are absent (Kolb and Tanaka 2001). Also, the domical shape of a planum-wide SPLD layer indicates the local influence of the buried Promethei basin rim on SPLD form, the late development of spiral troughs, and the lack of significant SPLD flow (Byrne and Ivanov 2004).

Here, we analyze SPLD sequences within the canyon and trough areas of Promethei Lingula. We use MOLA topographic data (115 m/pixel) and MOC high-resolution (4-11 m/pixel) images from the MGS spacecraft and moderately high-resolution (18-36 m/pixel) THEMIS visible images from the ODY spacecraft. MOC and THEMIS images were acquired from the NASA Planetary Data

Systems web site and processed using the USGS Integrated Software for Imagers and Spectrometers (ISI5

S). The MOLA topography was acquired from the USGS Planetary GIS Web Server (PIGWAD). Co-registered MOLA, MOC and THEMIS data were used to determine SPLD bedding orientations by solving 3-point problems for prominent SPLD layers. Our analysis addresses the following questions: What controlled SPLD bedding attitudes and canyon and trough development? When did canyon and trough formation occur relative to SPLD accumulation? How are other surface features related? What are the broader implications for SPLD history?

Geology of Promethei and Ultimum Chasmata

These canyons are >300 km long, a few tens of kilometers wide, and locally approach 2000 m in depth. Both chasmata have rugged floors exposing Hesperian and Noachian materials beneath the SPLD (Figure 2). Overall, the Planum Australe 1 unit beds appear to be fairly uniform in thickness, and brittle or ductile deformation structures resolvable in presently available data appear to be rare. THEMIS visible images of the chasmata walls reveal bedding unconformities at a consistent position within the Planum Australe 1 unit (Figure 2 and Supporting Figure 1). The unconformities have lengths between several to a few tens of kilometers and all are located in either the heads of the chasmata or where the SPLD abuts pronounced ridges in the substrate. These local unconformities are the expression of an inferred, regional contact that is otherwise apparently conformable in image data. The contact divides the unit into lower and upper members (units Aa_{1a} and Aa_{1b}, respectively; Figure 2). Typically, the unconformities result where unit Aa_{1b} rests on inferred erosional surfaces inclined into the chasmata. These surfaces are beds of unit Aa_{1a} that mantle gently sloping substrate topography (A-A' in Figure 2). Generally, unit Aa_{1a} is >300 m thick in chasma wall exposures and may exceed 1000 m in thickness away from the chasmata, whereas unit Aa_{1b} generally is a few to several hundred meters thick (Figure 2).

A large ridge of Noachian material (unit Npl_2) in the northwestern part of Promethei Chasma has ~600 m of relief above Hesperian material (unit Hdc). On the southeastern side of the ridge, traceable beds in unit Aa_{1a} in the lower parts of the chasma walls rise tens to nearly 200 m across distances of several to ~25 km as they approach the ridge. Lower beds are discontinuous where they pinch out against the large ridge as well as some smaller ones. On the northeast side of the ridge, the lower beds are flatter. In MOLA data of Ultimum Chasma, Australe 1 unit beds are generally indistinct or buried by the Planum Australe 2 unit, and substrate relief is modest, so bedding attitudes relative to the substrate cannot be determined.

The accumulation of units Aa_{1a} and Aa_{1b} generally produced fairly conformable mantling that subdued steeper slopes. However, more rapid subdual of some steeper northwest-facing slopes during deposition of the upper member is evident where some of the beds appear to lie nearly horizontal and/or pinch out upslope. Assuming that prevailing winds traveled northwestward down Planum Australe, this development indicates that Promethei Chasma initially developed more so on the southeast flank of the

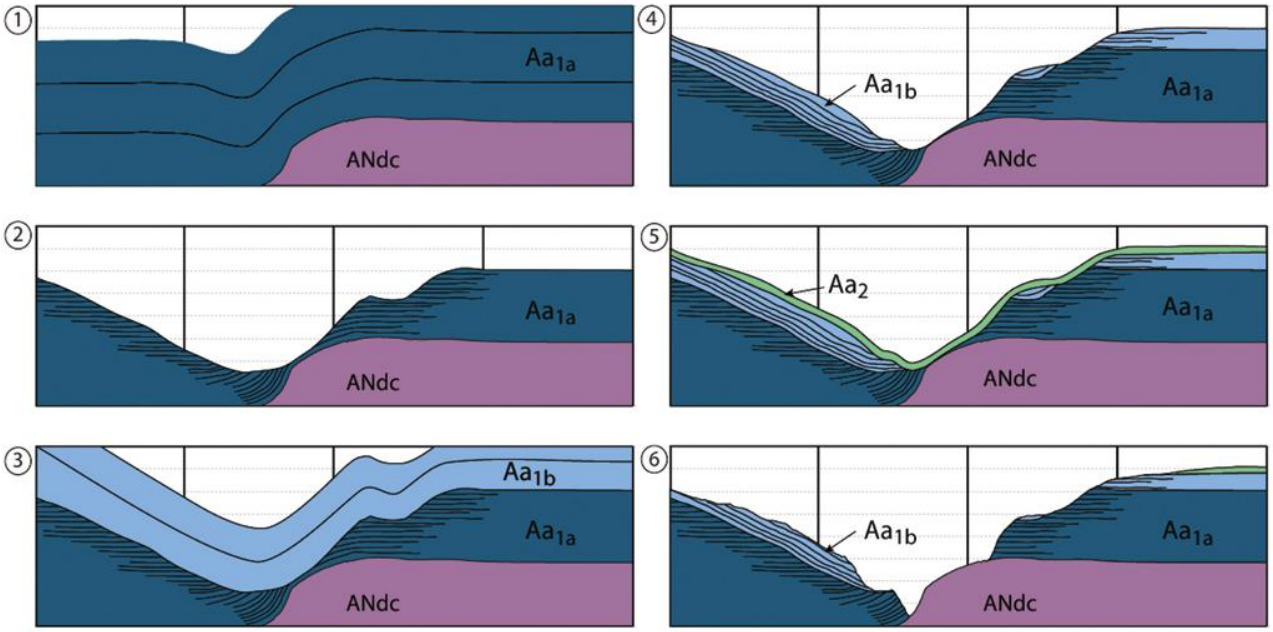

Figure 3. Cartoon showing formation history of Promethei Chasma along A-A' of Figure 2. Solid lines indicate bedding attitudes. Initial surface depressions (e.g., first panel) formed where SPLD mantled uneven substrate topography. Surface depressions form seedling chasmata that were widened and deepened during subsequent periods of sustained aeolian erosion (e.g., panel 2, 4, and 6) and renewed SPLD deposition (e.g., panel 3 and 5). (figure3.jpg)

broad ridge than on the northwest side, forming a "seedling canyon" capable of funneling and concentrating directional winds into it. Ultimum Chasma also may have had a seedling canyon upwind of a broad ridge in unit Npl_2 that crests ~100 km below its present head. Additional seedling canyons may have developed upwind and alongside other exposed substrate ridges and scarps that cross or bound outer parts of the chasma floor; such outer seedling canyon development may have been further promoted by winds funneled by up-slope seedling canyons.

The regional unconformity between the Planum Australe 1a and 1b units indicates that SPLD deposition was punctuated by a regional erosional event. In central Ultimum Chasma (Figure 2), unit Aa_{1a} was removed from part of the chasma floor and from parts of the canyon walls, particularly near cross-canyon ridges in the substrate, prior to unit Aa_{1b} deposition. This erosion effectively widened, locally deepened, and perhaps lengthened the seedling canyons. This event may reflect intensified, off-pole katabatic winds that interrupted otherwise fairly steady SPLD accumulation.

Renewed down-cutting followed deposition of unit Aa_{1b}, resulting in much of the form of the present chasmata. This stage of erosion also produced a northeast-trending trough cut in the Planum Australe 1 unit between the chasmata and connecting pronounced northwest-facing scarps within the chasmata floors (Figure 2). The trough has an equator-facing scarp nearly 700 m high, compared with a pole-facing scarp <200 m high. The trough extends northeast of Ultimum Chasma an additional 60 km. The trough may have formed initially in the Planum Australe 1a unit by topographically controlled insolation and winds and perhaps saltating particles that developed once the substrate topography was exhumed by erosion of the Planum Australe 1a unit and additionally after deposition of the Planum Australe 1b unit. Next, the chasmata were mantled by thin Planum Australe 2 unit beds that unconformably overly Planum Australe 1 beds. This unit later was largely removed from the chasmata walls and floors by recent and perhaps on-going wind action. Also, the marginal scarp of Promethei Lingula displays unmantled Planum Australe 1 unit, indicating erosion there is recent as well.

The overall history of the chasmata indicates three major stages of SPLD accumulation punctuated by two intense erosional hiatuses (e.g., Figure 3). A concentric trough formed during the second hiatus. Aeolian erosion interacting with substrate topography and perhaps saltating particles along with insolation-induced weathering likely is responsible for chasmata development. However, materials underlying the SPLD lack significant degradation of impact crater and ridge forms as well as aeolian flutes and yardangs, indicating that those materials were not susceptible to insolation weathering and wind erosion.

Geology of Australe Sulci canyon

The broad canyon that includes Australe Sulci (Figure 1) is ~440 km in length, averages 85 km in width, and is enclosed by walls that locally approach 1000 m in height. The canyon's floor descends >500 m along its axis, swings westward, and terminates above the eastern scarp of Chasma Australe. Within Australe Sulci, we identify six successive SPLD sequences whose subdivision is based on their topographic expression (cliff vs. terrace forming; Figure 4) and bounding marker beds. The sequences are laterally continuous for >150 km along canyon walls and across the canyon (except where the S3 sequence pinches out). Individual sequences are a few 10s to >150 m thick; total thickness of the exposed sequences is several hundred meters. The sequences exhibit gently undulating beds having wavelengths >10 km, both in cross- and down-canyon orientations; maximum bedding dips are <3.0°. The Australe Sulci canyon forms within a broad low in the bedding (B-B' in Figure 4). These sequences are all at much higher elevation than the base of unit Aa_{1b} defined in the nearby chasmata and thus are entirely within that upper unit.

The floor and western scarp of Australe Sulci is incised by numerous grooves that parallel the canyon trend. The grooves are typically hundreds of meters to >2000 m wide and 1 km to tens of kilometers long and are separated by ridges with similar dimensions. The grooves mostly occur in dense, closely spaced sets forming the sulci topography that overprints all the Planum Australe units in this area. In sequences S2 and S4, sulci are limited to a specific SPLD layer, whereas in sequences such as S1 and S3, sulci incise multiple layers.

A series of sinuous, east-trending, asymmetric ridges transect Australe Sulci. They are tens of kilometers long, up to several kilometers wide, spaced tens of kilometers apart, and exhibit less than a few 10s of meters of local relief. In places, sections of the ridges are degraded or removed, and, in others, they are overprinted with sulci. In MOC and THEMIS visible images, SPLD sequences are always exposed on the steeper, south-facing side of a ridge segment and in all instances MOLA topography indicates that the layers have a gentle northward apparent dip—in parallel with subjacent SPLD sequences (C-C' in Figure 4; Supporting Figure 2). We do not find folding of strata within these features as proposed by Koutnik et al. (2005).

The lower section of Australe Sulci canyon intersects a series of spiral troughs partly infilled by Planum Australe 2 unit (Figure 5). Here, several enclosed depressions aligned in series along the canyon floor cut into the spiral troughs' floors and equator-facing scarps. The depressions result in a stair-step, ridge-and-swale profile that mimics that of the unmodified, adjacent spiral troughs (X-X' and Y-Y' in Figure 5). The bottoms of cross-canyon spiral troughs are hundreds of meters lower than the crests of adjacent ridges and SPLD beds at the bases of the spiral troughs form the upper beds exposed in the canyon floor. Along the canyon floor, several circular and elongated mounds having kilometer-diameter bases and 10s to >100 m of relief (Figure 5; see also Supporting Figure 3) occur in resistant SPLD sequences. Enhanced grooves of the sulci extend down-canyon from some of the mounds (Figure 5). Within the

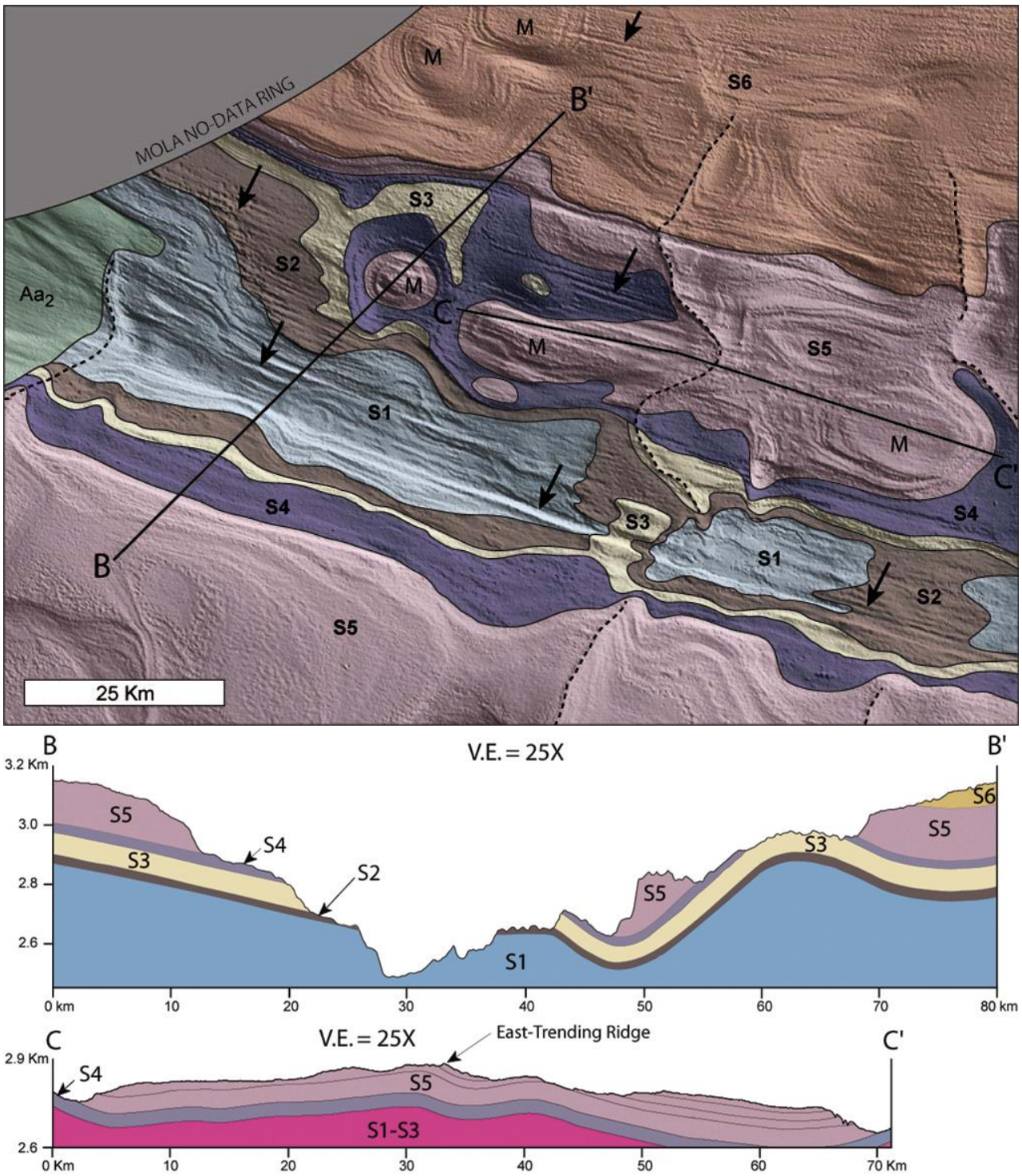

Figure 4. Geologic map and cross-sections of Australe Sulci. Here, Planum Australe 1b unit is subdivided into sequences S1 through S6 based on cliff-and-terrace morphologic characteristics. Sinuous, asymmetric ridges (dashed lines), circular plateaus (M), and curvilinear grooves or sulci (arrows). Maximum bedding dips are <3.0°. (figure4a.jpg, figure4b.jpg)

spiral troughs, SPLD sequences exposed in equator-facing scarps are laterally continuous and uniformly thick; bedding planes are nearly flat and devoid of layer pinch-outs and angular unconformities. Within Figure 5, spiral trough modification features include: (1) A broad, streamlined ridge, (2) preserved impact craters <1 km in diameter on equator-facing scarps, and (3) longitudinal grooves (sulci).

The Australe Sulci canyon results from the removal of >500 m of SPLD (unit Aa_{1b}) focused in a broad trough defined in SPLD bedding (Figure 4). The sulci that overprint the

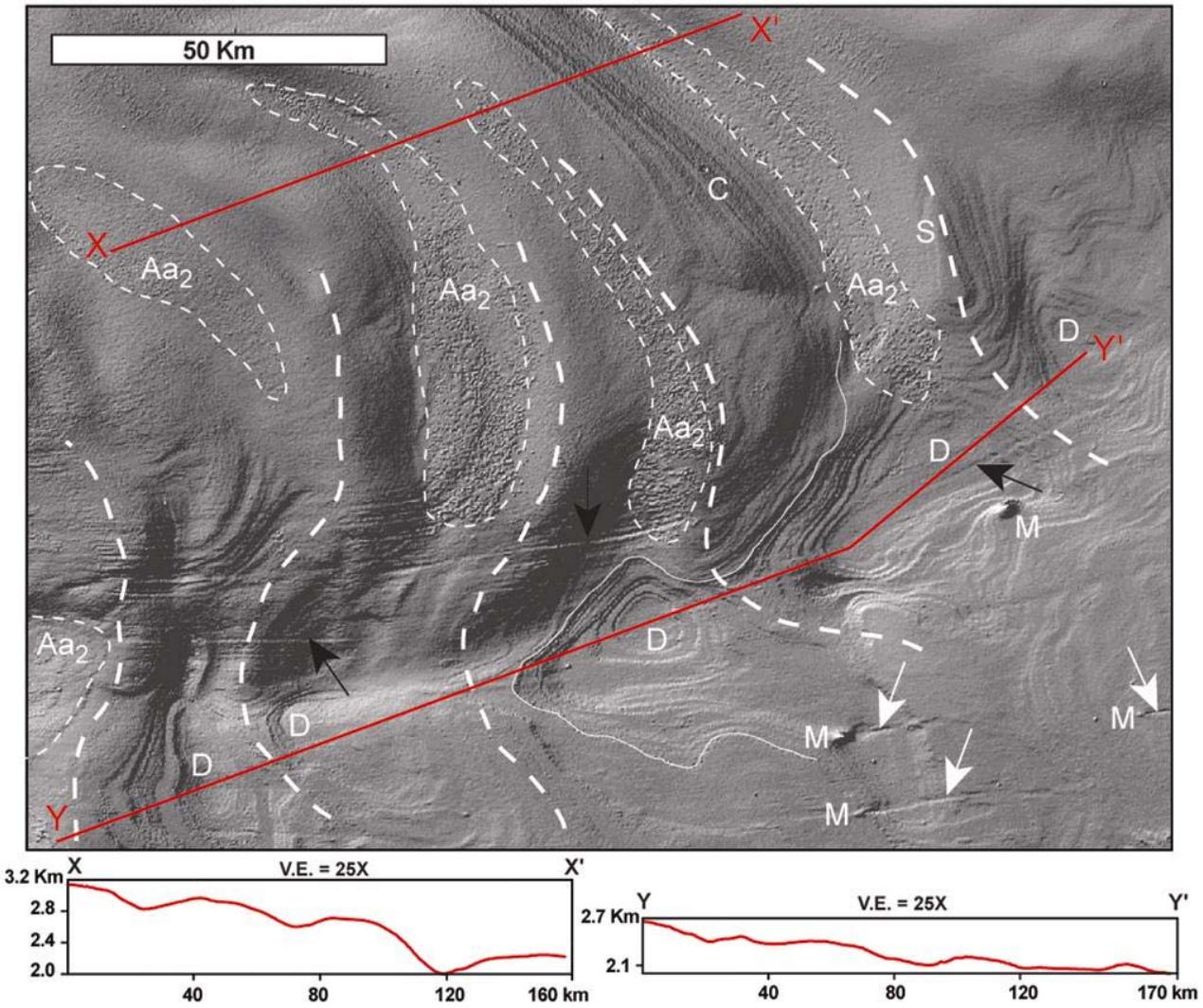

Figure 5. Northwest section of Australe Sulci canyon and adjacent spiral troughs exposing Planum Australe 1b unit except where superposed by Planum Australe 2 unit (outlined by thin dashed lines), which is continuous on floors of spiral troughs. Inter-trough ridges = thick dashed lines, D = depressions, S = streamlined ridge, M = mounds, arrows = sulci grooves (white where trailing mounds), trace of a particular terrace = solid line). Topographic profiles compare transects of spiral troughs (X-X') and ridge-and-swale features on Australe Sulci canyon floor (Y-Y'). (figure5.jpg)

sequences indicate surficial stripping most likely by off-pole katabatic winds (Koutnik et al. 2005). We propose that a more intense, earlier episode of the same process carved the canyon. The SPLD cliff-and-terrace topography is consistent with variable competency in the SPLD that may be caused by intra-layer ice/dust ratio variations, dust mantles overlying ice (Koutnik et al. 2005), or variable dust induration. Furthermore, we propose that aeolian erosion of variably competent and gently tilted SPLD sequences is responsible for formation of (1) circular plateaus made up of resistant SPLD carved within bowl-shaped bedding forms, and of (2) sinuous, asymmetric ridges as cuestas formed by undermining by wind of tilted beds capped by a resistant layer (Figure 4). Lastly, we interpret the small circular mounds (Figure 5) as remnants of SPLD impact ejecta that apparently were made more resistant to eolian erosion by impact-related processes. The hardening process is uncertain without more detailed knowledge of the makeup of the SPLD and the mounds. Some possibilities include melting and refreezing of fine-grained ice into coarser-grained ice, conversion of low-pressure ice into high-pressure polymorphs, and intimate mixing and alteration of SPLD dust and ice components. One mound contains a summit crater and occurs near several other mounds and impact craters (Supporting Figure 3b); these are similar to features identified closer to the south pole in Viking images (Herkenhoff and Murray 1992).

Uneven depositional surfaces and/or modest settling and tilting of SPLD over irregular topography may explain the dipping beds. For example, Byrne and Ivanov (2004) demonstrated that Promethei impact basin affected bedding attitudes in Australe Lingula west of the study region. The SPLD substrate in the Australe Sulci area may include rugged terrain as preserved within the floors of Promethei and Ultimum Chasmata. In addition, the erosional hiatus

between units Aa_{1a} and Aa_{1b} documented in the nearby chasmata also may have produced a seedling canyon system in underlying SPLD. In any case, the beds tilting into Australe Sulci (see B-B' in Figure 4) formed a shallow canyon that may have later funneled katabatic winds into it, thereby resulting in the present, deeper canyon and the longitudinal grooves, circular plateaus, sinuous ridges, and mounds within it.

Synthesis of geologic activity

Both the Australe Sulci canyon and the spiral troughs were largely formed during the erosional episode between deposition of the Planum Australe 1b and Planum Australe 2 units. Also, these units appear to be marked by sulci that are better developed in the Planum Australe 1b unit, indicating that sulci formation probably was associated with canyon development and continued modestly following Planum Australe 2 unit emplacement. The canyon and troughs may have formed together. The lack of substantial unconformities in the Planum Australe 1b unit indicates that the spiral troughs formed in place; we observe no evidence for lateral migration, although preferential widening of troughs in certain directions may have occurred.

The Planum Australe 2 unit layers appear heavily deflated, forming pitted sheets that grade into isolated mounds with increasing degradation. The unit is better preserved on flatter surfaces, including spiral trough floors and plateau tops (Figs. 1 and 5). Although the expression of Planum Australe 1 unit layering is evident in MOLA data across the Australe Sulci canyon and in adjacent spiral troughs, THEMIS and MOC images show that locally the layers appear to be mantled by a lag deposit consisting of bumpy debris that partly obscures the Planum Australe 1 unit. This lag deposit probably consists of highly deflated remnants of the Planum Australe 2 unit.

Deflation following emplacement of Planum Australe 2 unit largely has not affected the Planum Australe 1 unit, which is consistent with the preservation of pristine impact craters on spiral trough walls made up of the Planum Australe 1 unit. These relations indicate that post- Planum Australe 2 unit winds, perhaps assisted by insolation-driven weathering, eroded SPLD only along the most pronounced topography--the steepest and tallest walls of the chasmata and the margin of Planum Australe, in trends both radial and concentric to the polar plateau.

Overall, the period of erosion between Planum Australe 1b and 2 units appears to be responsible for the majority of erosion of Promethei Lingula, and perhaps the entire Planum Australe, resulting in the plateau margins, chasmata, and spiral troughs.

Directory of Supporting Data

root directory
- kolb_mars_2006_0001.pdf this file
- Fig. 1 figure1.jpg full-resolution image
- Fig. 2 figure2a.jpg, figure2b.jpg full-resolution image
- Fig. 3 figure3.jpg full-resolution image
- Fig. 4 figure4a.jpg, figure4b.jpg full-resolution image
- Fig. 5 figure5.jpg full-resolution image
- Supporting Fig. 1 sfigure1.j pg full-resolution image; sfig1.html figure description
- Supporting Fig. 2 sfigure2.jpg full-resolution image; sfig2.html figure description
- Supporting Fig. 3 sfigure3.jpg full-resolution image; sfig3.html figure description

Acknowledgements

We thank Shane Byrne and Ken Herkenhoff for their helpful comments during the preparation of this manuscript. This research was supported by NASA's Planetary Geology and Geophysics Program.

References

Clifford, S. M. (1987) "Polar basal melting on Mars" Journal of Geophysical Research 92, 9135-9152.

Byrne, S. and A. B. Ivanov (2004) "Internal structure of the Martian south polar layered deposits" Journal of Geophysical Research 109, E11001. doi:10.1029/2004JE002267

Fisher, D. A. (1993) "If martian ice caps flow: Ablation mechanisms and appearance" Icarus 105, 501-511. doi: 10.1006/icar.1993.1144

Head, J. W. (2000) "Evidence for geologically recent lateral migration of volatile-rich polar layered deposits" Second International Conference on Mars Polar Science and Exploration, August 21–25, 2000, Reykjavik, Iceland, LPI Contribution No. 1057.

Herkenhoff, K. E. and B. C. Murray (1992) "Geologic map of the MTM -90000 area, Planum Australe region of Mars" United States Geological Survey Miscellaneous Investigations Series, Map I-2304, scale 1:500,000.

Herkenhoff, K. E. and J. J. Plaut (2000) "Surface ages and resurfacing rates of the polar layered deposits on Mars" Icarus 144, 243-253. doi:10.1006/icar.1999.6287

Howard, A. D. (1978) "Origin of the stepped topography of the martian poles" Icarus 34, 581-599. doi:10.1016/0019-1035(78)90047-7

Howard, A. D. (2000) "The role of eolian processes in forming surface features of the martian polar layered deposits" Icarus 144, 167-288. doi:10.1006/icar.1999.6305

Kolb, E. J. and K. L. Tanaka (2001) "Geologic history of the polar regions of Mars based on Mars Global Surveyor data: II. Amazonian Period" Icarus 154, 22-39. doi:10.1006/icar.2001.6676

Koutnik, M. R., S. Byrne, and B. C. Murray (2002) "South polar layered deposits of Mars: The cratering record" Journal of Geophysical Research 107, E11, 5100 doi:10.1029/2001JE001805

Koutnik, M. R., S. Byrne, B. C. Murray, A. D. Toigo, and Z. A. Crawford (2005) "Eolian controlled modification of the martian south polar layered deposits" Icarus 174, 490-501. doi:10.1016/j.icarus.2004.09.015

Mellon, M. T. (1996) "Limits on the CO_2 content of the martian polar deposits" Icarus 124, 268-279. doi:10.1006/icar.1996.0203

Tanaka, K. L. and D. H. Scott (1987) "Geologic map of the polar regions of Mars" United States Geological Survey Miscellaneous Investigations Series, Map I-1802-C, scale 1:15,000,000.

Tanaka, K. L. and E. J. Kolb (2001) "Geologic history of the polar regions of Mars based on Mars Global Surveyor

data: I. Noachian and Hesperian Periods" Icarus 154, 3-21, doi:10.1006/icar.2001.6675

Tanaka, K. L. and E. J. Kolb (2005) "Geologic mapping of the polar regions of Mars: Preliminary results and climate implications" In U.S. Geological Survey Open-file Report 2005-1271 (T.K.P. Gregg et al., editors.) 47-48.

Thomas, P., S. Squyres, K. Herkenhoff, A. Howard, and B. Murray (1992) "Polar deposits of Mars" In Mars (H. H. Kieffer, B. M. Jakosky, C. W. Snyder and M. S. Mathews editors) 767-795, University of Arizona Press, Tucson.